The Plant Cell, Vol. 28: 1078–1093, May 2016, www.plantcell.org

Feedback Regulation of DYT1 by Interactions with Downstream bHLH Factors Promotes DYT1 Nuclear Localization and Anther Development

Jie Cui,[a,b] Chenjiang You,[a,b] Engao Zhu,[a,b] Qiang Huang,[a] Hong Ma,[a,b,c,1] and Fang Chang[a,b,1]

[a] State Key Laboratory of Genetic Engineering and Collaborative Innovation Center for Genetics and Development, School of Life Sciences, Fudan University, Shanghai 200438, China

[b] Ministry of Education Key Laboratory of Biodiversity Sciences and Ecological Engineering and Institute of Biodiversity Sciences, Institute of Plant Biology, School of Life Sciences, Fudan University, Shanghai 200438, China

[c] Center for Evolutionary Biology, Institutes of Biomedical Sciences, Fudan University, Shanghai 200438, China

ORCID ID: 0000-0001-8717-4422 (H.M.)

Transcriptional regulation is one of the most important mechanisms controlling development and cellular functions in plants and animals. The *Arabidopsis thaliana* bHLH transcription factor (TF) DYSFUNCTIONL TAPETUM1 (DYT1) is required for normal male fertility and anther development and activates the expression of the *bHLH010*/*bHLH089*/*bHLH091* genes. Here, we showed that DYT1 is localized to both the cytoplasm and nucleus at anther stage 5 but specifically to the nucleus at anther stage 6 and onward. The bHLH010/bHLH089/bHLH091 proteins have strong nuclear localization signals, interact with DYT1, and facilitate the nuclear localization of DYT1. We further found that the conserved C-terminal BIF domain of DYT1 is required for its dimerization, nuclear localization, transcriptional activation activity, and function in anther development. Interestingly, when the BIF domain of DYT1 was replaced with that of bHLH010, the DYT1^{N}-bHLH010^{BIF} chimeric protein shows nuclear-preferential localization at anther stage 5 but could not fully rescue the *dyt1-3* phenotype, suggesting that the normal spatio-temporal subcellular localization of DYT1 is important for DYT1 function and/or that the BIF domains from different bHLH members might be functionally distinct. Our results support an important positive feedback regulatory mechanism whereby downstream TFs increase the function of an upstream TF by enhancing its nucleus localization through the BIF domain.

INTRODUCTION

Rapid and precise spatial-temporal transcriptional regulation in all organisms promotes various biological processes and allows survival in different environments. Plants cannot move and have therefore developed complex transcriptional regulatory networks to respond to constantly changing conditions. In *Arabidopsis thaliana*, 6% (1717/28775) of all genes encode transcription factors (TFs), in contrast to only 3% in *Drosophila melanogaster* and 5% in humans (Pires and Dolan, 2010). One of the biggest TF families in Arabidopsis is the basic helix-loop-helix (bHLH) family, which contains 158 members (Pires and Dolan, 2010).

Plant bHLH proteins play important roles in many developmental processes, including anther development (Zhang et al., 2006; Feng et al., 2012; Fu et al., 2014; Gu et al., 2014; Zhu et al., 2015), stomata development (Kanaoka et al., 2008; Bhave et al., 2009; Nadeau, 2009; Serna, 2009b, 2009a), hormone signaling (Friedrichsen et al., 2002; Zhang et al., 2009), and light responses (Castillon et al., 2007; Leivar et al., 2008; Liu et al., 2008; Shin et al., 2009; Zhang et al., 2013). TFs can form heteromeric complexes that increase their combinatorial spectrum and specificity for distinct binding sites in both animals and plants (Lamb and McKnight, 1991; Zhao et al., 2008). Members of the bHLH family form both homodimers and heterodimers (Zhu et al., 2015), and different dimers could recognize different E-boxes and regulate distinct cellular processes.

In addition, bHLH TFs form feed-forward regulatory loops to control the complex and precise gene expression patterns in both Arabidopsis and rice (*Oryza sativa*) (Niu et al., 2013; Zhu et al., 2015). For instance, Arabidopsis DYSFUNCTIONL TAPETUM 1 (DYT1), which was the first bHLH transcription factor reported to specifically regulate the development and function of the tapetum, is required for the normal expression of ~1000 anther genes, of which 276 have been proposed to be affected by the feed-forward regulatory loops between DYT1 and the downstream bHLH TFs bHLH010, bHLH089, and bHLH091. DYT1 physically interacts with these three functionally redundant downstream bHLH TFs, which together modulate the expression of these 276 overlapping genes (Zhu et al., 2015). In rice, the expression of *TAPETUM DEGENERATION RETARDATION* (*TDR*) is activated by TDR INTERACTING PROTEIN2 (TIP2), which physically interacts with TDR, and they together form a feed-forward regulatory loop in the tapetum programmed cell death and pollen formation processes (Niu et al., 2013; Fu et al., 2014). However, the molecular mechanism underlying this feed-forward regulatory loop remains elusive.

In addition, because TFs bind to DNA and regulate gene expression transcriptionally, members of different TF families in plants, such as bHLH, MYB, and MADS, are thought to localize in

[1] Address correspondence to fangchang@fudan.edu.cn or hongma@fudan.edu.cn.

The author responsible for distribution of materials integral to the findings presented in this article in accordance with the policy described in the Instructions for Authors (www.plantcell.org) is: Fang Chang (fangchang@fudan.edu.cn).

www.plantcell.org/cgi/doi/10.1105/tpc.15.00986

the nucleus. However, some TFs are known to experience regulated localization, such as Os-MADS29, which is important for embryonic development and grain filling. Os-MADS29 shows conditional nuclear distribution in vivo through interactions with different MADS proteins (Nayar et al., 2014), but further details of the conditional nuclear distribution of MADS29 are not available. Posttranslational regulation through modulating the translocation of an already expressed TF from the cytoplasm to the nucleus is an efficient strategy for rapidly responding to developmental or stress signals.

In this study, we showed that DYT1 is localized to the nucleus in an anther stage-dependent manner and provided strong evidence for positive regulation of DYT1 by the downstream TFs bHLH010/bHLH089/bHLH091 through the enhanced nuclear localization of DYT1. In addition, we found that a plant-specific C-terminal domain, named the BIF domain, is required for the heterodimerization of DYT1 with bHLH010/bHLH089/bHLH091. In conclusion, the results strongly support a positive feedback regulatory loop in which the DYT1-downstream TFs bHLH010/bHLH089/bHLH091 positively regulate DYT1 function by enhancing the nuclear localization of DYT1 through BIF domain-dependent heterodimerization with DYT1.

RESULTS

The Transcription Factor DYT1 Showed Stage-Dependent Nuclear Localization

As one of the gatekeeper TFs required for tapetum development, DYT1 is specifically expressed in tapetal cells (Gu et al., 2014). Previously, we showed (Feng et al., 2012) that expression of DYT1 in the cytoplasm as a fusion to the ligand binding domain of the glucocorticoid receptor (GR) failed to rescue the *dyt1-1* mutant, with few pollen grains, but the translocation of DYT1-GR into the nucleus due to the treatment with the glucocorticoid hormone analog dexamethasone restores male fertility of *ProDYT1:DYT1-GR/dyt1-1* plants. These results were reproduced by the dexamethasone induction of DYT1-GR in the *dyt1-3* mutant background (Supplemental Figure 1), indicating that DYT1 functions in the nucleus during anther development.

To examine detailed subcellular localization of DYT1 during the anther developmental processes, we observed the *DYT1-EYFP* distribution from anther stage 4 to 7 (Sanders et al., 1999) using the *ProDYT1:DYT1-EYFP/dyt1-3* transgenic line. We found that (1) DYT1 was expressed faintly in the center of each anther lobe at anther stage 4 and that expression increased in level and became specific to tapetal cells at anther stage 5-7 (Figure 1A); (2) DYT1 was localized to both the cytoplasm and nucleus at early anther stage 5 but was distributed more in the nucleus at later anther stage 5 and was nuclear-specific at anther stage 6 and onward (Figures 1A to 1C; Supplemental Figure 2A), suggesting that DYT1 localization is regulated temporally. We further analyzed the average amounts of DYT1 fluorescence in the cytoplasm or nucleus relative to the total amount in the cell at anther stages 5-7 using the LAS X Microsoft program from Leica, and the statistical analysis results also confirmed the increased nuclear localization and reduced cytoplasmic distribution of DYT1 in tapetal cells as anther development progressed (Supplemental Figure 2). These results prompt the question of how the stage-dependent distribution pattern of DYT1 is regulated during anther development.

DYT1 Interacts with Multiple bHLH Proteins, and Their Heterodimers Show Nuclear Localization

To identify the factors that potentially affect DYT1 localization and function, we performed a yeast two-hybrid (Y2H) screen of an Arabidopsis cDNA library using DYT1 as the bait and obtained 358 clones encoding 143 candidate DYT1-interacting proteins, including 30 TFs and proteins predicted to function in protein synthesis and degeneration, signaling, hormone metabolism, and development (Supplemental Figure 3 and Supplemental Data Set 1). When we retested their interactions in plants using bimolecular fluorescence complementation (BiFC), we found that the YFP signals that indicated the interaction between DYT1 and bHLH010, bHLH089, bHLH091, bHLH033/ICE2, bHLH057, bHLH116/ICE1, and bHLH125 were strongly and specifically localized to the nucleus, unlike the signal of the DYT1 homodimer, which was predominantly located in the cytoplasm and only weakly in the nucleus (Figure 1D; Supplemental Data Set 2). These results suggested that heterodimer formation increased the nuclear distribution of DYT1. We showed recently that *bHLH010*, *bHLH089*, and *bHLH091* are highly expressed in the anther with similar patterns, later than *DYT1*, and that they function downstream of *DYT1* (Zhu et al., 2015). This finding, together with the localization results, led us to postulate that the protein products of the DYT1-downstream genes *bHLH010*, *bHLH089*, and *bHLH091* act as positive feedback regulators of DYT1 activity by promoting DYT1 nuclear localization.

We hypothesized that the different localization patterns of DYT1 homo- and heterodimers can be explained by at least two possible mechanisms: (1) As in the case of APETALA3 and PISTILLATA (McGonigle et al., 1996), both DYT1 and DYT1-interacting bHLHs have a weak or bipartite nuclear localization sequence (NLS); they alone were predominantly located in the cytoplasm but enter the nucleus after they form heterodimers. (2) DYT1 possesses a weak NLS and depends on a partner for strong nuclear localization, whereas each of its interaction partners has a strong NLS for nuclear localization without DYT1.

To test these possibilities, we first determined the subcellular localization of DYT1-interacting bHLHs in a transient expression system in tobacco leaves and found that bHLH010, bHLH089, and bHLH091 exhibited strong and specific nuclear localization patterns (Figure 1E; Supplemental Data Set 2), which supported the second hypothesis that the DYT1-interacting bHLHs facilitate DYT1 nuclear translocation. Next, we expressed EYFP-tagged DYT1 alone or in combination with each of the bHLH proteins to test the effect of bHLH010/bHLH089/bHLH091 on DYT1 localization. As expected, DYT1-EYFP was predominantly distributed in the cytoplasm, with only a relatively weak signal in the nucleus; however, the same protein strongly and specifically localized to the nucleus when coexpressed with bHLH010, bHLH089, or bHLH091 (Figure 1F; Supplemental Data Set 2), demonstrating that all three DYT1-downstream interacting proteins promoted the nuclear localization of DYT1.

DYT1 Contains a Conserved Domain (BIF) Required for Dimerization

To investigate the potential functional domain that is required for the dimerization and translocation of DYT1, we performed

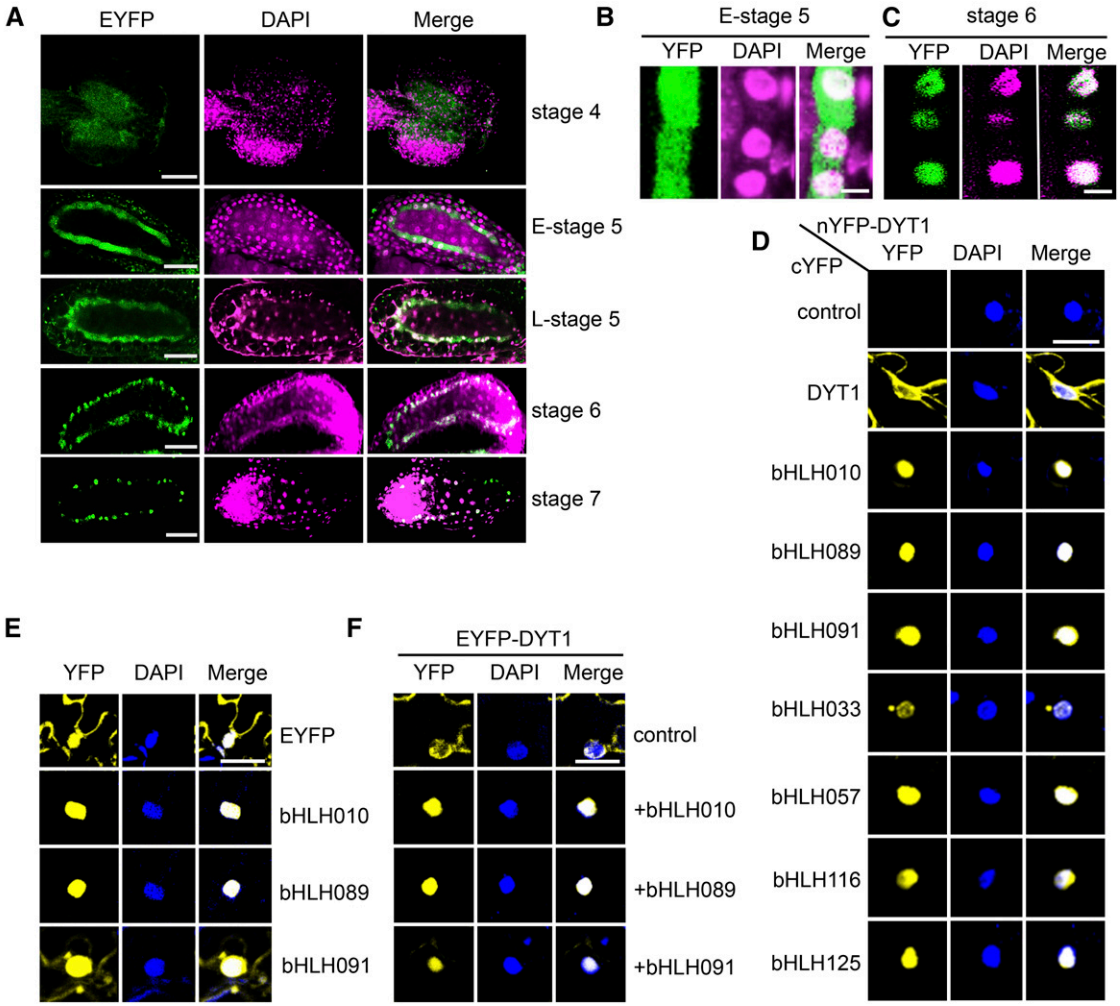

Figure 1. The Subcellular Localization of DYT1 in Arabidopsis Anthers and Various DYT1 Dimers in Tobacco Leaves.

(A) The subcellular localization of DYT1-EYFP in Arabidopsis tapetal cells at anther stage 4-7. Images show longitudinal sections of anthers.
(B) and **(C)** The enlarged tapetal cells at early anther stage 5 (Sanders et al., 1999) (E-stage 5; **[B]**) and anther stage 6 **(C)**. Green shows the EYFP signals from the DYT1-EYFP fusion proteins, magenta shows the DAPI-stained nuclei, and white shows the merged signals from YFP and DAPI.
(D) The subcellular localization of DYT1 homodimer and different heterodimers.
(E) The subcellular localization of the three DYT1-interaction proteins: bHLH010, bHLH089, and bHLH091.
(F) The localization of DYT1-EYFP in the control or bHLH010/089/091 coexpression background. Yellow shows the signal from YFP, blue indicates the DAPI-stained nuclei, and white represents the merged signals from YFP and DAPI.
Bar = 25 μm in **(A)**, 3 μm in **(B)** and **(C)**, and 20 μm in **(D)** to **(F)**.

secondary structure predictions using the PredictProtein website (https://www.predictprotein.org) and found that DYT1 had a predicted ββαββα topology in the C-terminal region (Supplemental Figure 4; Figure 2A), which we named the bHLH protein interaction and function (BIF) domain after we determined its role in DYT1 activity. Other than DYT1, 59 of 158 Arabidopsis bHLH genes harbor this domain (Supplemental Data Sets 3 and 4). Moreover, although it could not be identified using the HMM method from the Pfam database, the domain with the characteristic secondary structure is widely found in bHLH genes in other plant species. For example, there are 32 genes encoding proteins containing the BIF domain in *Amborella trichopoda*, the sister species of all other extant angiosperms. This suggested that this domain might have conserved functions during evolution.

In general, the function of bHLH TFs relies on two aspects: their binding to target DNA sequences and their dimerization with various partners, with the latter being essential for increasing the combinatorial spectrum of distinct binding sites (Lamb and McKnight, 1991; Zhao et al., 2008). Therefore, we tested whether the BIF domain is also required for DNA binding. We showed previously that DYT1 could bind in vitro to conserved G-box sequences (TCACGTGA) (Feng et al., 2012). Therefore, we generated two truncated versions of DYT1, DYT1$^{\Delta BIF}$ (amino acids 1 to 124) and DYT1^{BIF} (amino acids 125 to 207) (Figure 2A), and tested

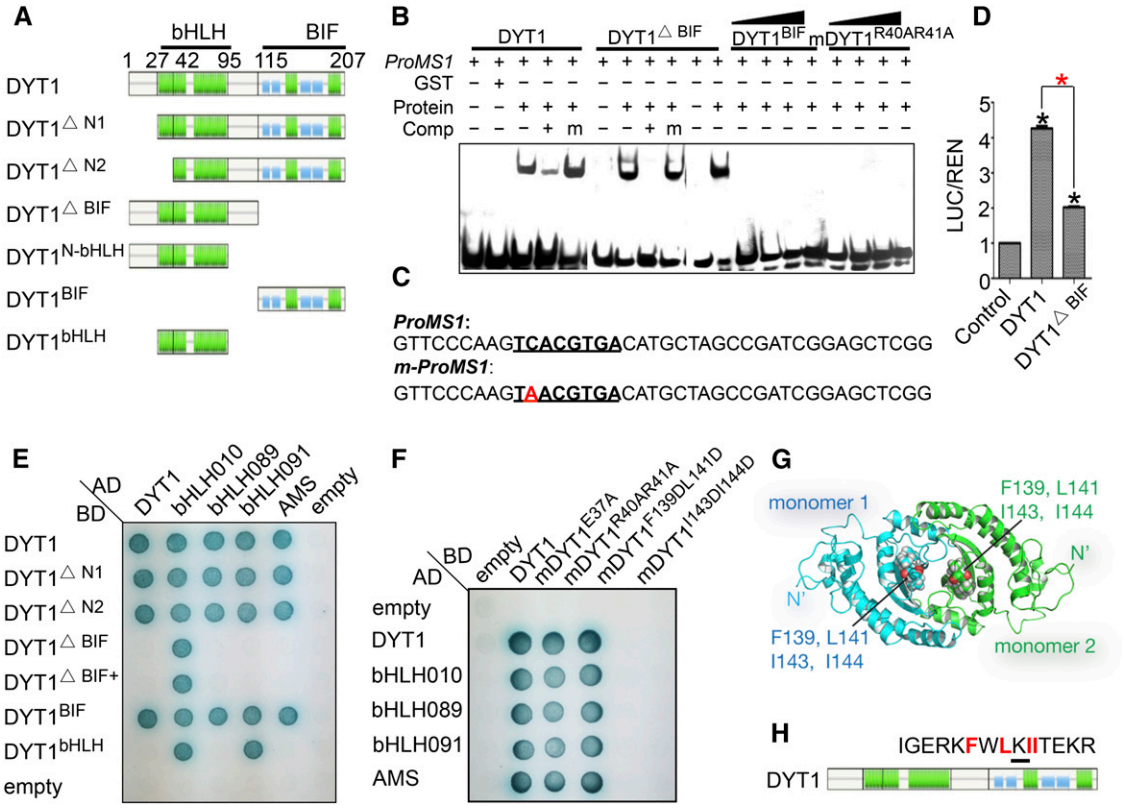

Figure 2. Y2H and EMSA Analyses to Determine the Motif and Amino Acids Critical for DYT1 DNA Occupation and Dimerization.

(A) Schematic diagram to show the length and domains in full-length DYT1 and DYT1 truncations. Green and blue boxes represent β-sheets and α-helices, respectively.

(B) EMSA of binding of various truncated and mutant DYT1 forms to the G-box in the *MS1* promoter region (*ProMS1*). DYT1 with mutations in the bHLH basic region (mDYT1^{R40AR41A}) was used as a negative control.

(C) DNA sequence of probes used in the EMSA. *ProMS1*, positive probe; m-*ProMS1*, competition probe with mutation. The core G-box sequence is underlined, and the mutated nucleotide is indicated in red.

(D) Relative reporter activity (LUC/REN) of DYT1 and DYT1$^{\triangle BIF}$ on the *MS1* promoter. Empty vector was used as the control. The black asterisks indicate a statistically significant difference from the control, and the red asterisk indicates a significant difference between full-length DYT1 and DYT1$^{\triangle BIF}$ ($P < 0.01$, *t* test). Error bars indicate SD of the biological replicates, $n \geq 3$.

(E) Interactions between truncated DYT1 and DYT1, bHLH010, bHLH089, bHLH091, and AMS. Blue indicates positive protein-protein interactions.

(F) Interactions between DYT1, bHLH010, bHLH089, bHLH091, and AMS with DYT1 carrying point mutations. Expression of DYT1 and DYT1 mutant proteins in the Y2H system is shown in Supplemental Figure 6.

(G) The predicted 3D structure of DYT1^{BIF} homodimer. Four amino acids (i.e., F139, L141, I143, and I144) are shown in red.

(H) Schematic of full-length DYT1 showing the location of F139, L141, I143, and I144 in the BIF domain. The amino acid sequence of the black line-labeled part was shown above, and the red fonts indicated F139, L141, I143, and I144.

the binding of these two proteins to the G-box target sequence to investigate whether the BIF domain is required for DNA binding (Figure 2B). Using the G-box sequence of the *MS1* promoter as a probe (Figure 2C), we found that the negative control protein mDYT1^{R40AR41A}, in which the conserved basic region was mutated, exhibited absolutely no DNA binding ability (Figure 2B). However, the BIF domain deletion showed no obvious defect in the DNA binding ability of DYT1, and the BIF domain alone did not bind to the DNA probe (Figure 2B). These data demonstrated that the bHLH motif, but not the BIF domain, is required for the direct G-box occupation of DYT1. Interestingly, when we compared the function of DYT1 and DYT1$^{\Delta BIF}$ to activate *MS1* transcription using a transient transcription assay system (Hellens et al., 2005; Liu et al., 2008), we found that DYT1$^{\Delta BIF}$ (Figure 2A) showed a dramatic reduction in transcriptional activity (Figure 2D), suggesting that the BIF domain is important for the in vivo function of DYT1.

We then tested whether the BIF domain is required for DYT1 dimerization. Various truncated versions of DYT1, including DYT1$^{\Delta N1}$ (amino acids 27 to 207), DYT1$^{\Delta N2}$ (amino acids 42 to 207), DYT1$^{\Delta BIF}$ (amino acids 1 to 124), DYT1 $^{N\text{-}bHLH}$ (amino acids 1 to 95), DYT1^{BIF} (amino acids 125 to 207), and DYT1^{bHLH} (amino acids 27 to 95), were generated (Figure 2A) and used to detect whether they retained the ability to form homo- and heterodimers. As shown in Figure 2E, deletion of the BIF domain (DYT1$^{\Delta BIF}$) abolished DYT1 homodimerization and its interactions with bHLH089, bHLH091, or ABORTED MICROSPORES (AMS), but

did not obviously affect the interaction with bHLH010. The BIF domain alone (DYT1^{BIF}) interacted with all four bHLH proteins (Figure 2E), suggesting that the BIF domain is necessary and sufficient for DYT1 to interact with itself, bHLH089, bHLH091, and AMS, whereas the bHLH domain is not important for this process. However, for interactions with bHLH010, either the bHLH motif or the BIF domain was sufficient. Similarly, BiFC experiments in tobacco leaves showed that DYT1^{BIF} interacted with itself, bHLH010, bHLH089, or bHLH091, but that DYT1$^{\Delta BIF}$ did not interact with bHLH089 or bHLH091 (Supplemental Figure 5). These results suggested the importance of the BIF domain for DYT1 dimerization.

BIF Domain Residues F139, L141, I143, and I144 Are Important for DYT1 Dimerization

To further investigate which residues are critical for the function of the BIF domain, 16 amino acids conserved among DYT1 orthologs in the BIF domain were chosen for site-directed mutagenesis (Supplemental Figure 4), with mutations of four individual conserved amino acids in the bHLH domain as controls, including mDYT1^{E37A} and mDYT1^{R40AR41A}. We reasoned that, if a residue is important for dimerization, a mutation that changes its chemical property dramatically, such as from acidic to basic, should weaken DYT1 dimerization. We generated full-length DYT1 constructs with mutations and tested their dimerization ability. The E37A and R40AR41A mutations in the bHLH region did not obviously affect either DYT1 homodimerization or heterodimerization with bHLH010, bHLH089, bHLH091, or AMS (Figure 2F); these results were consistent with the results of the bHLH deletion and suggested again that the BIF domain but not the bHLH motif is essential for DYT1 dimerization. However, two double mutants (mDYT1^{F139DL141D} and mDYT1^{I143DI144D}; Figures 2G and 2H) showed neither DYT1 homodimerization nor heterodimerization (Figure 2F; Supplemental Figure 6), indicating that residues 139, 141, 143, and 144 are important for DYT1 dimerization. The expression of the mutant DYT1 proteins in yeast was detected using immunoblot analysis, and the results showed that these proteins were expressed at similar levels as wild-type DYT1, indicating that the negative interaction results were not caused by reduced or absent expression of proteins (Supplemental Figure 7).

To explore why these amino acid sites were important for DYT1 dimerization, we predicted the 3D structure of the DYT1^{BIF} homodimer. As illustrated in Figure 2G, we found that there are eight hydrophobic residues, including F139, L141, I143, and I144, in each monomer, of two DYT1 ^{BIF} monomers contacting closely to form a hydrophobic core in the center of the homodimer. This suggests that the interaction between two BIF domains might be driven mainly by the hydrophobicity of these residues. Thus, amino acid alterations of these interface residues leading to reduced hydrophobicity of the side chains might disrupt the DYT1 protein-protein interactions, consistent with our observations (Figure 2F).

BIF-Mediated Heterodimerization Is Required for DYT1 Nuclear Localization in Anthers

Having shown that the nuclear localization of DYT1 is dependent on interactions with bHLH partners, we hypothesized that point mutations in the BIF domain that abolished DYT1 heterodimerization would also affect DYT1 nuclear localization. We first tested this hypothesis using BiFC in tobacco leaves. Unlike wild-type DYT1, which specifically localized to the nucleus when coexpressed with bHLH010, bHLH089, or bHLH091 (Figure 1F), the mDYT1^{F139DL141D} and mDYT1^{I143DI144D} mutant proteins were distributed mostly in the cytoplasm, even when coexpressed with bHLH010, bHLH089, or bHLH091 (Figures 3A and 3B; Supplemental Data Set 2), thus indicating that heterodimerization is crucial for DYT1 nuclear localization.

To further test the effect of the point mutations on DYT1 localization and function in Arabidopsis anther cells, constructs expressing C-terminally EYFP-tagged DYT1$^{\Delta BIF}$, mDYT1^{F139DL141D}, and mDYT1^{I143DI144D} driven by the *DYT1* native promoter were generated and transformed into the *dyt1-3*/+ heterozygous background. The presence of various *DYT1* transgenes was verified in each T1 transgenic line, and lines heterozygous for the T-DNA insertional *dyt1-3* allele were identified. These T1 transgenic plants in the *dyt1-3*/+ background were named as follows: Line-A#, DYT1-EYFP lines; Line-B, DYT1^{BIF}-EYFP lines; Line-C#, DYT1$^{\Delta BIF}$-EYFP lines; Line-D#, mDYT1^{F139DL141D}-EYFP lines; and Line-E#, mDYT1^{I143DI144D}-EYFP lines. For each line in the *dyt1-3*/+ background, the T2 progeny with a 3:1 segregation ratio for the newly introduced transgene (insensitive:sensitive to hygromycin for the marker in the new T-DNA constructs) were planted for further studies. The expression level of *DYT1-EYFP*, *DYT1^{BIF}-EYFP*, *DYT1$^{\Delta BIF}$-EYFP*, *mDYT1^{F139DL141D}-EYFP*, and *mDYT1^{I143DI144D}-EYFP* in the T2 transgenic generation in the *dyt1-3* homozygous background was analyzed (Supplemental Figure 8), and Line-A1, Line-B1, Line-C1, Line-D1, and Line-E1 showed a similar *DYT1/mDYT1* expression level to the native *DYT1* in the wild-type plant. Therefore, Line-A1, Line-B1, Line-C1, Line-D1, and Line-E1 in the *dyt1-3* background were chosen for further phenotypic investigations and the T2 progeny in the wild-type background from the same T1 transgenic lines were used for further in vivo protein localization analyses.

As expected, unlike DYT1, which showed a nuclear-specific distribution pattern at anther stage 6 and onward (Figures 1A, 1C, and 3C), the fluorescent signals in Line-C1/WT (DYT1$^{\Delta BIF}$-EYFP), Line-D1/WT (mDYT1^{F139DL141D}-EYFP), and Line-E1/WT (mDYT1^{I143DI144D}-EYFP) were widely distributed in the cytoplasm of tapetal cells and were detected in the nucleus only weakly at either anther stage 6 or stage 7 (Figures 3D to 3F), confirming that the same BIF domain sites required for DYT1 dimerization are critical for its nuclear distribution in tapetal cells. These results together demonstrated that the BIF domain is important for the nuclear localization of DYT1 and strongly support the idea that heterodimerization facilitates the presence of DYT1 in the nucleus at relatively high levels.

The BIF Domain Is Essential for DYT1 Function and Transcriptional Activation Activity in Vivo

We next explored whether the BIF domain is required for DYT1 in vivo function by determining whether the defective anther development was rescued by the expression of *DYT1^{BIF}-EYFP*, *DYT1$^{\Delta BIF}$-EYFP*, *mDYT1^{F139DL141D}-EYFP*, or *mDYT1^{I143DI144D}-EYFP* in the above-mentioned Line-B1/*dyt1-3*, Line-C1/*dyt1-3*,

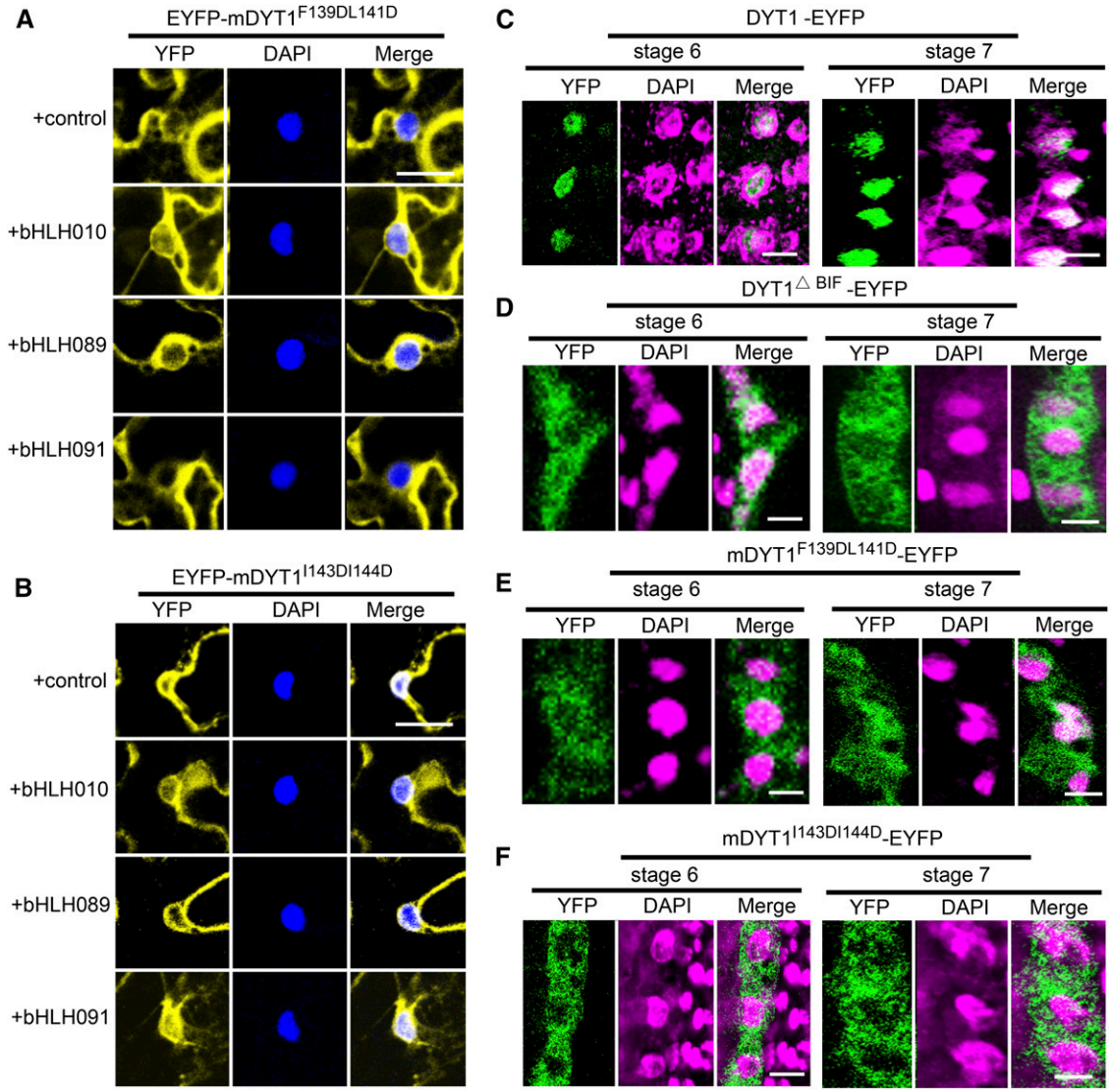

Figure 3. Deletion and Mutations in the BIF Domain Disturbing the Protein Interactions Also Affect the Nuclear Localizations.

(A) and **(B)** The subcellular localization of mDYT1^{F139DL141D} and mDYT1^{I143DI144D} alone or when coexpressed with bHLH010/089/091. Yellow shows the signal from YFP, blue indicates the DAPI-stained nucleus, and white represents the merged signals from YFP and DAPI. Bars = 20 μm.

(C) to **(F)** The subcellular localization of DYT1-EYFP (Line-A1/*dyt1-3*), DYT1$^{\triangle BIF}$-EYFP (Line-C1/WT), mDYT1^{F139DL141D}-EYFP (Line-D1/WT), and mDYT1^{I143DI144D}-EYFP (Line-E1/WT) in Arabidopsis tapetal cells at anther stage 6 and stage 7. Green indicates EYFP signals, and magenta shows the DAPI-stained cell nucleus. Bars = 3 μm.

Line-D1/*dyt1-3*, and Line-E1/*dyt1-3* transgenic lines. The *dyt1-3* mutant is male sterile and lacks pollen grains. The expression of *DYT1-EYFP* fully restored a normal phenotype to the *dyt1-3* mutant because all identified Line-A#/*dyt1-3* plants produced normal siliques and pollen, similar to wild-type plants (Line-A1/*dyt1-3*; Figure 4; Supplemental Data Set 5). By contrast, all detected Line-B#/*dyt1-3*, Line-C#/*dyt1-3*, Line-D#/*dyt1-3*, and Line-E#/*dyt1-3* plants, including Line-B1/*dyt1-3*, Line-C1/*dyt1-3*, Line-D1/*dyt1-3*, and Line-E1/*dyt1-3*, showed defective anther development, similar to that of the *dyt1-3* mutant (Figure 4; Supplemental Data Set 5), suggesting that the BIF domain and the F139L141/I143I144 sites in the BIF domain are important for proper *DYT1* function in vivo.

The expression of *DYT1^{BIF}-EYFP* did not restore male fertility in the *dyt1-3* mutant (Line-B1/*dyt1-3*; Figure 4), indicating that the BIF domain alone is not sufficient for DYT1 function. Moreover, the *DYT1^{BIF}-EYFP* transgene in the wild-type background (Line-B1/WT) affected normal pollen development and produced defective pollen grains (Figure 4), suggesting a potential dominant-negative effect of the DYT1^{BIF} truncation. To test this idea, we observed the male fertility of 15 other *DYT1^{BIF}-EYFP*/WT (Line-B#/WT) transgenic lines. Among the 15 lines, six showed defective pollen

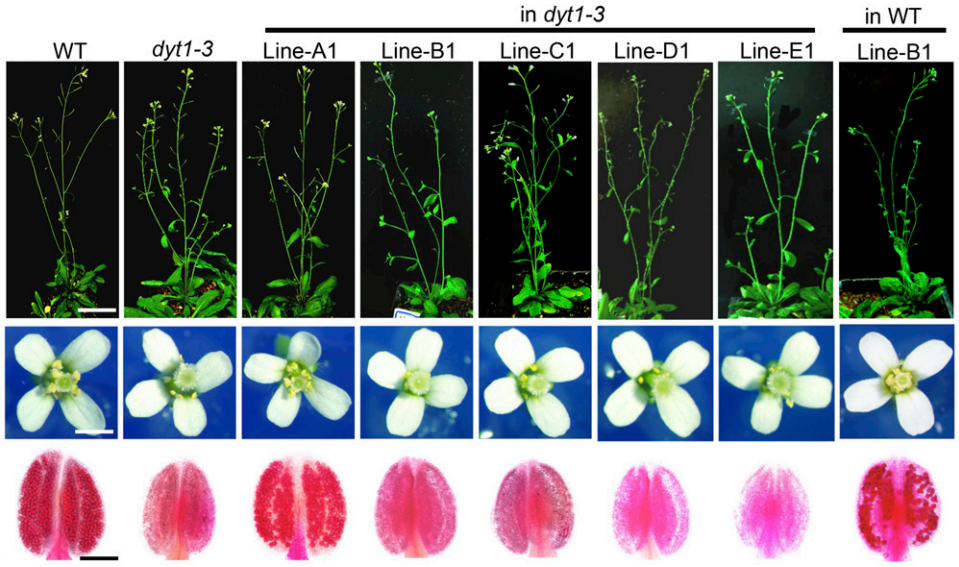

Figure 4. Phenotypic Analyses of Plant Growth, Flowers, and Anthers of the Wild-Type, *dyt1-3*, Line-A1/*dyt1-3*, Line-B1/*dyt1-3*, Line-C1/*dyt1-3*, Line-D1/*dyt1-3*, Line-E1/*dyt1-3*, and Line-B1/WT Plants.

Bar = 3 cm for plants (in the first panel), 500 μm for flowers (in the second panel), and 20 μm for anthers (in the third panel).

development as Line-B1/WT did. We further measured the *DYT1^{BIF}-EYFP* expression level in all the 15 *DYT1^{BIF}-EYFP*/WT lines (Supplemental Figure 9) and found that Line-B4/WT to Line-B9/WT, which exhibited reduced male fertility, showed a more than 2-fold *DYT1^{BIF}* expression level than the wild-type plant. However, the other nine lines that exhibited normal male fertility, including Line-B7/WT to Line-B15/WT, showed similar DYT1^{BIF} expression levels, close to that of the wild type (Supplemental Figure 9). These results confirmed the potential dominant-negative effect of the DYT1^{BIF} truncation, possibly because DYT1^{BIF} interfered with normal DYT1 function by interacting with the DYT1 partners.

As shown in Figures 3C to 3F, the mutant DYT1 proteins were preferentially localized in the cytoplasm but were also present at low levels in the nucleus. We examined whether the nuclear-localized mutant DYT1 proteins had any transcriptional activity by assessing the expression of DYT1-regulated TF genes, including *MYB35*, *MS1*, *MYB99*, *MYB103*/*MYB80*, and *AMS*, in transgenic Line-A1/*dyt1-3*, Line-B1/*dyt1-3*, Line-C1/*dyt1-3*, Line-D1/*dyt1-3*, and Line-E1/*dyt1-3* and compared their expression levels with those in wild-type and *dyt1-3* plants. We hypothesized that if the BIF domain and/or BIF domain-mediated dimerization were/was required for DYT1 transcriptional activation activity, the low level of mutant DYT1 proteins present in the nucleus would activate the expression of downstream genes, albeit not to the same extent as in the wild type or Line-A1/*dyt1-3*, but to a greater extent than in the *dyt1-3* mutant. However, the expression of *MYB35*, *MS1*, *MYB99*, *MYB103*/*MYB80*, and *AMS* in these mutant *DYT1* transgenic lines all showed no obvious difference to those in the *dyt1-3* mutant (Figures 5B to 5F), although the expression level of these mutant *DYT1* genes was similar to that of *DYT1* genes in wild-type and Line-A1/*dyt1-3* plants (Figure 5A), strongly suggesting that the BIF domain and the F139/L141/I143/I144 sites in the BIF domain that are important for the in vivo function of DYT1 are probably involved in both the nuclear distribution of DYT1 and the nuclear transcriptional activation activity of DYT1.

The DYT1-bHLH089 Heterodimer Specifically Activates *MYB35* Expression

Previous studies have revealed that DYT1 targets the promoters of *MS1* and *MYB35* (Feng et al., 2012; Gu et al., 2014). However, our in vivo transcriptional activation assay using the transient transcription assay system (Hellens et al., 2005; Liu et al., 2008) showed that DYT1 alone activates the expression of *MS1* and *MYB35* only moderately (LUC/REN<10) (Figures 6A and 6B). We propose that the low level of activation of *MS1* and *MYB35* expression by DYT1 in the transient system is because of the low level of DYT1 in the nucleus or that the normal expression of *MS1* and *MYB35* in the Arabidopsis anther might be activated by DYT1 heterodimers. We therefore tested the activation of *MS1* and *MYB35* expression induced by NLS-DYT1 fusion protein and various DYT1 heterodimers, such as DYT1-bHLH010, DYT1-bHLH089, and DYT1-bHLH091. *MYB35* was highly activated specifically by the DYT1-bHLH089 heterodimer, but not by either bHLH089 alone or NLS-DYT1 (Figure 6A), suggesting that the DYT1-bHLH089 heterodimer is required for high-level *MYB35* activation. By contrast, DYT1 alone, DYT1-bHLH010, DYT1-bHLH089, DYT1-bHLH091 heterodimers, and NLS-DYT1 all activated the expression of MS1 to similar levels (Figures 6A and 6B), suggesting that *MS1* could be activated by one of several DYT1 dimers. Curiously, although DYT1 heterodimers could somehow activate *MS1*, the expression of *MS1* in DYT1-EYFP transgenic plant Line-A1 (Figure 5) was not restored to the wild-type level. Perhaps the DYT1-EYFP fusion protein interacts less efficiently than the normal DYT1 protein with an unknown factor that is

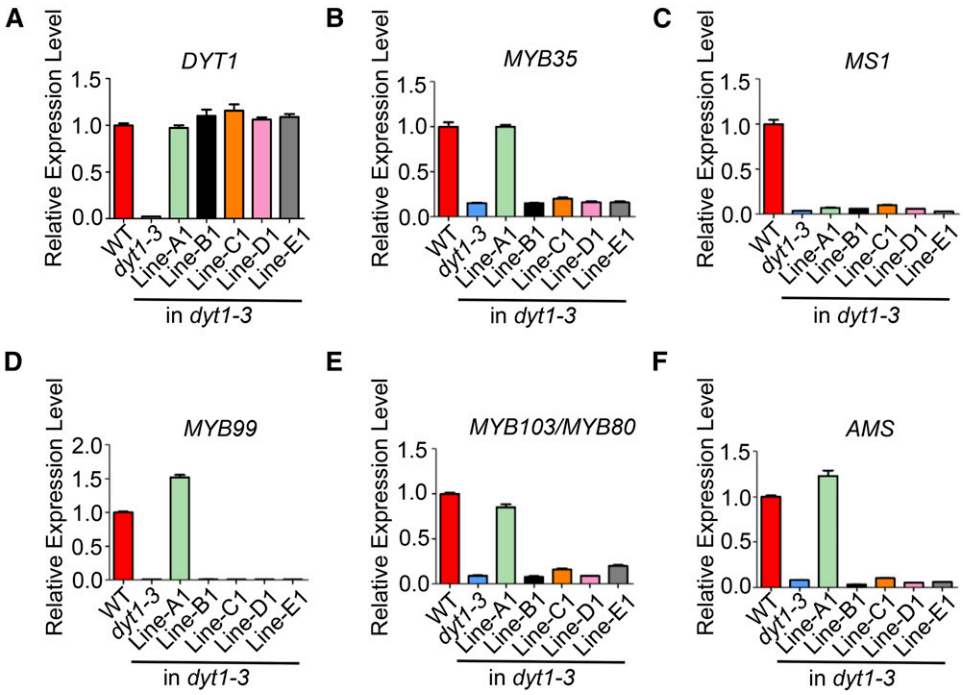

Figure 5. Real-Time PCR Analysis Showing the Relative Expression Levels of Detected DYT1-Downstream Genes in the Wild-Type, *dyt1-3*, and Different Transgenic Plant Inflorescences.

DYT1 **(A)**, *MYB35* **(B)**, *MS1* **(C)**, *MYB99* **(D)**, *MYB103*/*MYB80* **(E)**, and *AMS* **(F)**. EF1α serves as the internal control. Error bars indicate SD of three technical repeats.

required for the activation of *MS1* expression. To determine whether the DYT1-bHLH089 heterodimer directly binds to the *MYB35* promoter, we performed in vitro DNA binding experiments using both DYT1 and bHLH089 proteins with the *MYB35* promoter sequences containing E-box motifs and found that the heterodimer could bind strongly (Figure 6D). Thus, the DYT1-bHLH089 protein complex probably activates *MYB35* expression due to the strong synergistic binding of the heterodimer to the *MYB35* promoter (Figure 6E).

In addition, the $DYT1^{\Delta BIF}$ truncated protein and DYT1 harboring F139DL141D or I143DI144D mutations minimally activated the expression of the *MYB35* reporter (Figure 6C), suggesting the importance of the BIF domain in DYT1 transcriptional activation activity. In addition, NLS-$DYT1^{\Delta BIF}$, NLS-$DYT1^{F139DL141D}$, and NLS-$DYT1^{I143DI144D}$, which all exhibited increased nuclear localization, did not show enhanced transcriptional activity of *MYB35* either alone or together with bHLH089 (Figure 6C), suggesting that, in addition to nuclear localization, the transcriptional activation activity of DYT1 also required the BIF domain and the F139DL141D/I143DI144D sites.

The BIF Domains of DYT1 and bHLH010/bHLH089/bHLH091 Contributed Differently to DYT1 Nuclear Localization and Function

Although belonging to the same bHLH TF family, DYT1 largely remained in the cytoplasm, whereas bHLH010, bHLH089, and bHLH091 individually showed strong nuclear localization (Figures 1D and 1E). To investigate the reason for this difference in nuclear localization of DYT1 and the three bHLH proteins, we compared the amino acid sequences of the four bHLH proteins. The predicted secondary structure of the BIF domain (ββαββα) was highly conserved in many plant bHLH proteins, but the amino acid sequences of the DYT1 BIF and the BIFs of bHLH010/089/091 showed substantial differences (Supplemental Figure 10A), suggesting possible functional differentiation of the BIF domain between different bHLH paralogs. Furthermore, the NLS prediction results from the cNLS mapper website (http://nls-mapper.iab.keio.ac.jp) revealed that in addition to an NLS in the bHLH motif, the bHLH010/bHLH089/bHLH091 proteins also contained a predicted weak NLS at the beginning of the BIF domain; however, DYT1 had no predicted NLS in the same region (Supplemental Figure 10B).

We then tested whether the BIF domains affected the nuclear distribution of these bHLH proteins. $bHLH010^{\Delta BIF}$ and $bHLH089^{\Delta BIF}$ both showed exclusively nuclear distributions; by contrast, $DYT1^{\Delta BIF}$ localized strongly in the nucleus and also in the cytoplasm (Figure 7A; Supplemental Data Set 2), suggesting that the DYT1 BIF domain might interfere with nuclear localization. In addition, the BIF domains of bHLH010 and bHLH089 localized preferentially to the nucleus, but the BIF domain of DYT1 was detected mostly in the cytoplasm (Figure 7B; Supplemental Data Set 2), revealing different properties of the distinct BIF domains. These results combined with the finding that DYT1 alone localized preferentially to the cytoplasm (Figures 1D and 1F) suggested that the DYT1 BIF domain may act as a switch that turns on the nuclear

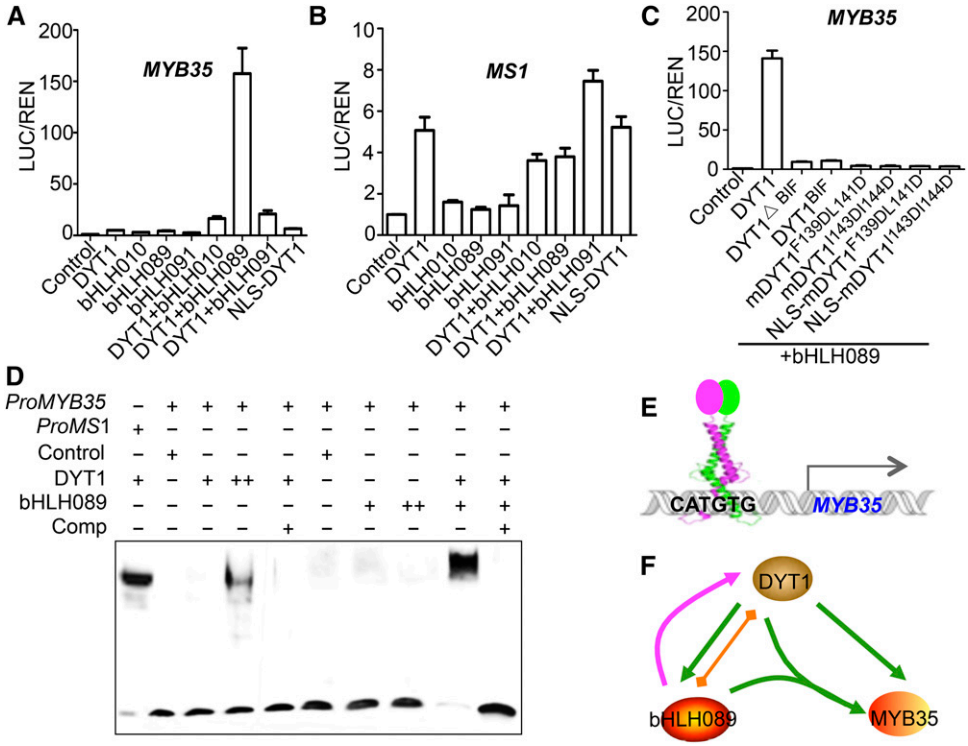

Figure 6. The BIF Domain Is Involved in the Transcriptional Specificity of Different DYT1 Heterodimers.

(A) and **(B)** Transcriptional activation of *MS1* and *MYB35* by dimers of DYT1 and bHLH proteins.
(C) Activation of *MYB35* by dimers of mutant DYT1 proteins and bHLH089. Transiently expressing blank vector and reporter serve as the control. The *y* axis shows relative reporter activity (LUC/REN). Error bars indicate SD of at least three biological repeats.
(D) EMSA using DYT1 and bHLH089 alone or in combination. The first lane shows the interaction between DYT1 and the E-box sequence of *ProMS1*, serving as the positive control. Comp, competition probe; ++, double the amount of protein as +.
(E) Proposed model in which the DYT1-bHLH089 heterodimer binds to the CATGTG E-box of *MYB35* promoter and activates the transcription of *MYB35*.
(F) DYT1 and bHLH089 regulate the expression of *MYB35* through both feed-forward and positive feedback regulatory loops. DYT1 somehow activates the expression of *bHLH089* and interacts with bHLH089 products and together they promote the expression of *MYB35*, thus forming a feed-forward loop. The downstream bHLH089 interacts with cytosolic DYT1 and increases DYT1 translocation to the nucleus; thus, bHLH089 positively regulates the activity of DYT1. Orange line indicates protein interaction, green arrows show transcriptional activation, and the magenta arrow implies a positive feedback regulation.

distribution of DYT1 by interacting with other nuclear-targeted bHLH TFs. In the absence of interactions with other bHLHs, DYT1 largely remained in the cytoplasm, ready to interact with its partners.

To further test this hypothesis, we constructed chimeric proteins that contained an N-terminal region from DYT1 ($DYT1^N$), including the bHLH motif, and a C-terminal region with the BIF domain from either bHLH010 ($bHLH010^{BIF}$) or bHLH089 ($bHLH089^{BIF}$) and analyzed the subcellular distribution of the chimeric proteins (Figure 7C). As predicted, the $DYT1^N$-$bHLH010^{BIF}$ and the $DYT1^N$-$bHLH089^{BIF}$ chimeric proteins exhibited nuclear-specific localization (Figure 7D; Supplemental Data Set 2), lacking detectable cytoplasmic signals. We next expressed $DYT1^N$-$bHLH010^{BIF}$ using the native *DYT1* promoter in the *dyt1-3* mutant background and examined their subcellular localization in the anther to test whether these chimeric proteins functioned as well as the native DYT1. Consistent with the transient expression results, $DYT1^N$-$bHLH010^{BIF}$ (Line#1; Supplemental Figure 11) was found to be already specifically localized to the nucleus of tapetal cells at anther stage 5, whereas wild-type DYT1 at this stage was still preferentially distributed in the cytoplasm of tapetal cells (Figures 7E and 7F).

Next, we investigated the in vivo function of $DYT1^N$-$bHLH010^{BIF}$ and $DYT1^N$-$bHLH089^{BIF}$ by testing whether they could rescue anther development in *dyt1-3*. Unlike the seven transgenic lines carrying the native promoter-driven wild-type *DYT1* that all recovered the anther development and fertility of the *dyt1-3* mutant, 2 of the 14 (14.3%) $DYT1^N$-$bHLH010^{BIF}$ transgenic plants and 11 of the 14 (78.6%) $DYT1^N$-$bHLH089^{BIF}$ transgenic plants showed defective anthers and sterile siliques (Figures 7G and 7H), although other chimeric transgenic plants showed normal fertility. As a control, we used real-time PCR to estimate the expression levels of the chimeras between the lines with reduced fertility and the wild-type DYT1 transgenic lines and found that the expression levels were comparable with or even higher than those in lines with normal fertility (Supplemental Figure 11). These results suggest that precocious nuclear localization of DYT1 might not be beneficial for DYT1 function; alternatively, the BIF domain of DYT1 might have unknown functions unrelated to nuclear localization but necessary

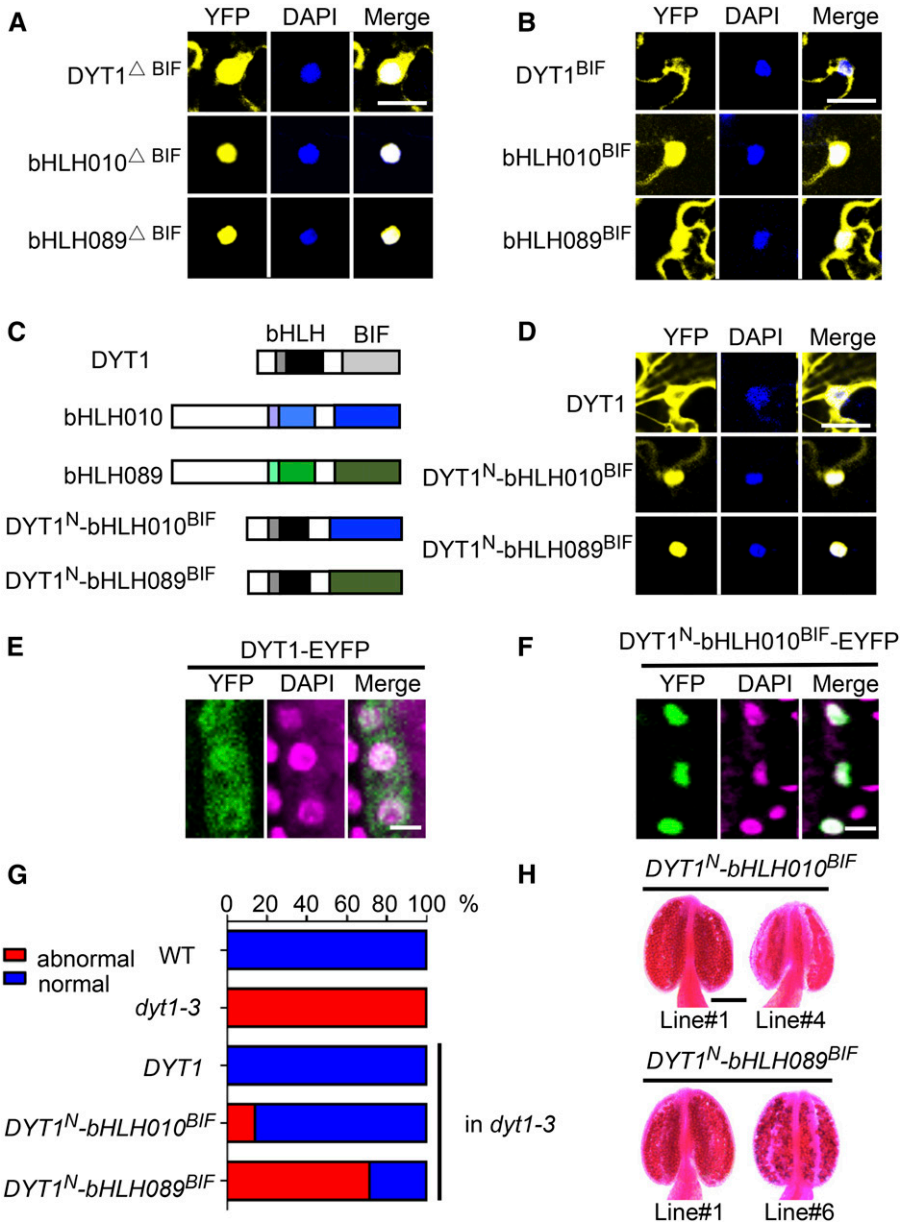

Figure 7. The BIF Domain Contributes to the Conditional Regulation of DYT1 Nuclear Distribution.

(A) The subcellular localization of DYT1$^{\Delta BIF}$, bHLH010$^{\Delta BIF}$, and bHLH089$^{\Delta BIF}$.
(B) The subcellular localization of the BIF domain from DYT1 (DYT1^{BIF}), bHLH010 (bHLH010^{BIF}), and bHLH089 (bHLH089^{BIF}).
(C) Schematic maps of DYT1, bHLH010, bHLH089, and the DYT1 chimeric proteins, which combined the N-terminal region of DYT1 (DYT1^{N}) with the BIF domain of bHLH010 (DYT1^{N}-bHLH010^{BIF}) or bHLH089 (DYT1^{N}-bHLH089^{BIF}). The gray box and the black box together show the bHLH domain of DYT1 (DYT1^{bHLH}), the light-purple box and light blue box together show bHLH010^{bHLH}, and the light-green box and green box together show bHLH089^{bHLH}. The light-gray box indicates DYT1^{BIF}, the dark-blue box indicates bHLH010^{BIF}, and the dark-green box indicates bHLH089^{BIF}. The first white box in each protein represents amino acids before the bHLH domains, and the second white box in each protein is for amino acids between the bHLH domain and BIF domain.
(D) The subcellular localization of DYT1 and the two DYT1 chimeric proteins DYT1^{N}-bHLH010^{BIF} and DYT1^{N}-bHLH089^{BIF}. Bar = 20 μm.
(E) and **(F)** The subcellular distribution of DYT1-EYFP and DYT1^{N}- bHLH010^{BIF}-EYFP in Arabidopsis tapetal cells at anther stage 5. Bar = 3 μm.
(G) Statistical analysis of transgenic lines showed percentages of normal (blue) and abnormal (red) fertility in the *dyt1-3*, *DYT1*/*dyt1-3*, *DYT1^{N}-bHLH010^{BIF}*/*dyt1-3*, and *DYT1^{N}-bHLH089^{BIF}*/*dyt1-3* transgenic plants. The blue boxes represent transgenic lines with normal fertility, and the red boxes indicate plants with reduced fertility.
(H) Phenotypic analysis of anthers of the *DYT1^{N}-bHLH010^{BIF}*/*dyt1-3* and *DYT1^{N}-bHLH089^{BIF}*/*dyt1-3* transgenic lines. Bar = 20 μm.

for normal anther development, probably phosphorylation-related regulation.

DISCUSSION

Transcriptional regulation plays a critically important role in anther development, and several types of TFs regulate this important process, including the bHLH proteins DYT1, AMS, and bHLH010/bHLH089/bHLH091 from Arabidopsis and their rice homologs UNDEVELOPED TAPETUM1, TDR, TIP2, and ETERNAL TAPETUM1/DELAYED TAPETUM DEGENERATION (Sorensen et al., 2003; Jung et al., 2005; Zhang et al., 2006; Feng et al., 2012; Ji et al., 2013; Niu et al., 2013; Fu et al., 2014; Xu et al., 2014; Zhu et al., 2015). DYT1 acts as a gatekeeper of the complex transcriptional network that regulates tapetal and microspore development (Zhang et al., 2006; Feng et al., 2012; Zhu et al., 2015). Our results here on the functional domains of DYT1 and the effects of its interactions with three bHLH proteins have three important implications. First, our studies provided strong evidence supporting a positive feedback loop between the bHLH transcription factors in the regulation of anther development. Second, we provided mechanistic insights for regulating transcriptional activation activity, namely, the promotion of the localization of a TF from the site of its synthesis to the organelle of its function. Third, we discovered the conserved C-terminal BIF domain in many Arabidopsis bHLH proteins and revealed its critical role in mediating the physical interaction between DYT1 and bHLH010/089/091 and in the positive feedback regulation of DYT1 function.

Complex Transcriptional Networks in the Regulation of Anther Development

Our previous studies revealed that DYT1 and bHLH010/bHLH089/bHLH091 form a feed-forward loop that regulates the anther transcriptional network in which *bHLH010/089/091* were activated by DYT1 and some of their translation products form heterocomplexes with DYT1 and subsequently regulate the expression of many DYT1 target genes (Zhu et al., 2015). Although the molecular mechanisms through which DYT1 activates the transcription of *bHLH010/089/091* are not clear, our findings here uncovered an important mechanism that regulates the function of DYT1 through its increased nuclear distribution and also a novel positive feedback regulatory loop from the bHLH010/089/091 proteins to DYT1, supporting a working model for how DYT1 regulates anther development (Figure 8). *DYT1* is expressed at an early stage of anther development (late stage 4 to early stage 5), but the DYT1 homodimers have limited nuclear distribution, with most of the proteins remaining in the cytoplasm. The basal level of DYT1 in the nucleus could activate low-level expression of bHLH010/089/091, which then physically interacts with DYT1 and facilitates the nuclear localization of DYT1, so that *bHLH010/089/091* are increasingly expressed. This is entirely consistent with the results that *bHLH010/089/091* are expressed slightly later than DYT1 and in the same anther cell layers as DYT1 (Zhu et al., 2015). In addition to facilitating the nuclear localization of DYT1, different DYT1-bHLH heterodimers bind to the E-boxes of various downstream genes; for instance, the DYT1-bHLH089 complex binds to and activates the expression of *MYB35*, thereby activating the complex anther transcriptional networks. Thus, we reveal a mechanism by which the function of a TF is activated through its increased nuclear distribution due to interactions with its own downstream factors.

Interestingly, our previous studies also showed that the *DYT1* transcript level was increased in the *bhlh010/089/091* triple mutant compared with in the wild type (Zhu et al., 2015), suggesting negative feedback regulation of *DYT1* expression by bHLH010/089/091. We propose that at the early anther stage 5, low levels of bHLH010/089/091 proteins interact with DYT1 to enhance the nuclear localization and transcriptional activity of DYT1. As more bHLH010/089/091 are expressed, more DYT1-bHLH complexes are localized to the nucleus and regulate downstream genes. Afterward, a negative feedback regulatory pathway is directly/indirectly activated by bHLH010/089/091 to suppress the expression of *DYT1* and prevent excessive *DYT1* expression. Therefore, normal anther development and transcriptional networks are regulated by both positive and negative feedback loops to maintain stable levels.

One interesting result worth noting is that different interaction combinations of bHLH010/089/091 with DYT1 showed differential transcriptional activation of downstream genes (Figures 5A and 5B), although bHLH010, bHLH089, and bHLH091 have been shown to play redundant roles in the regulation of anther development (Zhu et al., 2015). These results suggested that these three bHLH duplicates possibly have distinct functions in the regulation of downstream anther genes, which are not easily detected through morphological analyses but could be identified by the more sensitive molecular phenotypic examination. Based on the differences in their amino acid sequences, their expression level, and the *cis*-elements in their promoter regions, we proposed possible functional differentiation of the *bHLH010/089/091* genes (Zhu et al., 2015), and we believe that further molecular phenotypic analyses of the single mutant of *bHLH010/089/091* will help to uncover the potentially distinct functions of these three genes in the regulation of anther development, as well as other processes.

The BIF Domain Is Required for DYT1 Function

In this study, we defined a BIF domain that is important for the physical interaction of bHLH proteins and DYT1 transcriptional activation activity. This domain is found in over one-third of Arabidopsis bHLH TF family members (Supplemental Data Set 3). The bHLH transcription factors usually function in dimer or tetramer form or by forming a complex with other TF family members (Ellenberger et al., 1994; Ma et al., 1994; Huffman et al., 2001; Li, 2014; Chang et al., 2015); often the bHLH motif is required for dimerization. In this study, we demonstrated that the plant-specific BIF domain is also important for the dimerization and the normal function of DYT1.

It is worth noting that the BIF domain of DYT1 and those of bHLH010/089/091 show different capabilities in multiple aspects, such as nuclear localization and in vivo functions (Figure 7). DYT1 and bHLH010/089/091 were derived from different ancestral genes that separated from each other as early as in the ancestor of vascular plants (Pires and Dolan, 2010), suggesting that the functions of the BIF domain in these proteins differentiated before the origin of floral structures, possibly because the specification of BIF functions in these proteins facilitated more precise regulation of

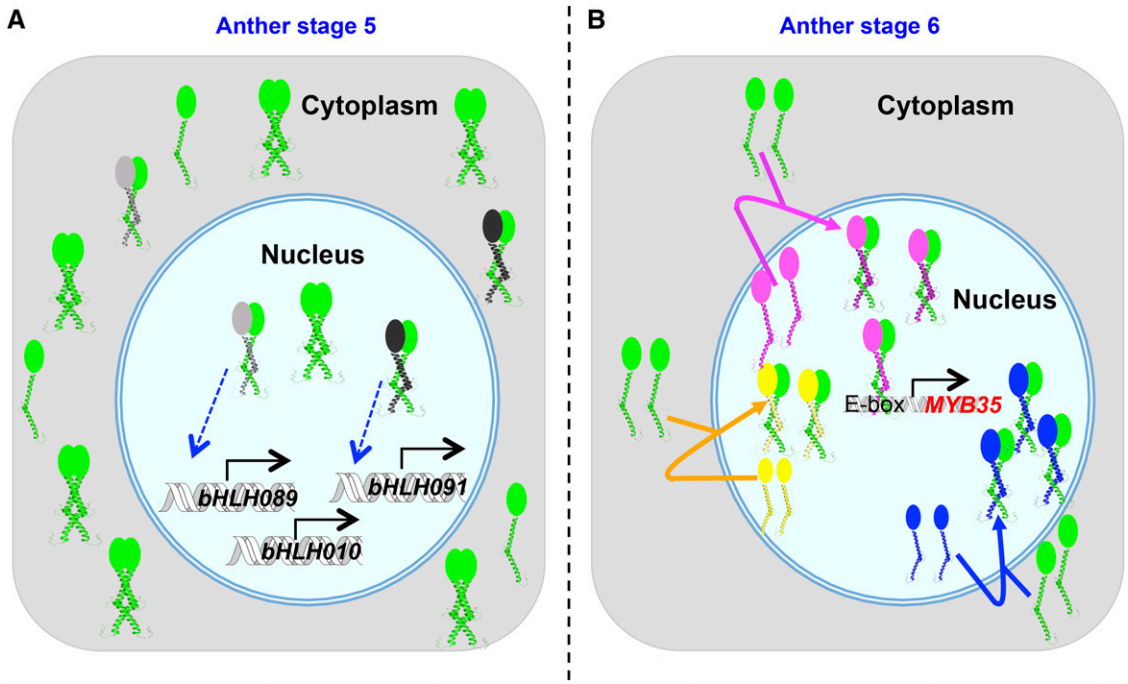

Figure 8. Proposed Working Model of DYT1-bHLH010/089/091 Transcriptional Regulatory Loops.

(A) DYT1 expression is initiated at early anther stage 5, and DYT1 monomers and homodimers do not localize to the nucleus. Some unknown factors (in gray and black) could interact with DYT1 and help some DYT1 translocate into the nucleus, and DYT1 then directly or indirectly activates the expression of bHLH010/089/091. bHLH transcripts are translated into proteins, which then interact with DYT1 to form heterodimers.
(B) The bHLH010/bHLH089/bHLH091 proteins interact with DYT1 and facilitate DYT1 nuclear localization, and DYT1-bHLH089 heterodimers bind to the E-box of *MYB35* and promote *MYB35* expression. Green indicates DYT1; yellow, bHLH010; magenta, bHLH089; and blue, bHLH091. Black lines and arrows show transcription; blue arrows with dotted lines show direct or indirect activation; the magenta arrow, the yellow arrow, and the blue arrow indicate the protein translocation from the cytoplasm to the nucleus; ovals in different colors all indicate BIF domains, and the two interacting bHLH motifs are shown as two coiled helices.

microsporogenesis. Furthermore, the phylogeny of the bHLH genes harboring the BIF domain implied a single origin of the BIF domain as well (Pires and Dolan, 2010). Although the BIF domains share a highly conserved $\beta\beta\alpha\beta\beta\alpha$ secondary structure, different BIF domains show relatively high degrees of amino acid sequence divergence, suggesting more functional differentiation of BIF domains, possibly in terms of protein partners, as compared with that of the bHLH domain, which has a highly conserved function of DNA binding.

Before the identification of the BIF domain here, the ACT domain was reported to be composed of four β-strands and two α-helixes arranged in a $\beta\alpha\beta\beta\alpha\beta$ fold, which is similar to the BIF domain ($\beta\beta\alpha\beta\beta\alpha$); the ACT domains are involved in the control of metabolism, solute transport, and signal transduction in bacteria (Grant, 2006). Despite the low level of amino acid sequence similarity between the ACT and BIF domains, it is possible that these two domains were somehow related in ancestral plants and then further diverged with specialized functions during the plant evolutionary history.

Various Nuclear Localization Regulation Mechanisms of Transcription Factors

As transcription factors regulate gene expression, their nuclear distribution is one of the necessary conditions for in vivo function. Previous studies have revealed multiple mechanisms that positively regulate the translocation of TFs from the cytoplasm to the nucleus. For instance, the brassinosteroid (BR)-responsive TFs BZR1/2 (brassinazole-resistant 1/2), which directly bind to DNA and regulate BR-induced gene expression, showed different distribution states in the presence or absence of BR signal. In the absence of BR, BZR1/2 are phosphorylated by the GSK3-like kinase BIN2 (BR-insensitive 2) and are excluded from the nucleus. In the presence of BR, BZR1/2 are dephosphorylated by an unknown mechanism, accumulate in the nucleus, and regulate the expression of BR-target genes (Kim et al., 2009). In addition, the Arabidopsis MADS proteins APETALA3 and PISTILLATA lack a functional NLS and are present in the cytoplasm when alone, but interact with each other and together are localized in the nucleus (McGonigle et al., 1996). In addition, the transcription factor bZIP28 associated with the endoplasmic reticulum (ER) is cleaved in response to treatment with tunicamycin, an agent that blocks N-linked protein glycosylation, and then releases its cytoplasm-facing domain for translocation into the nucleus (Liu et al., 2007). The ER-to-nucleus translocation of EIN2, a positive regulator of ethylene signaling, is then triggered by a phosphorylation-regulated proteolytic processing (Ju et al., 2012; Qiao et al., 2012).

Here, we revealed a novel mechanism for regulating the cytoplasm-to-nucleus translocation of TFs that involves physical interaction with its partners that have strong NLSs. Through the

physical interaction, three DYT1-downstream TFs, bHLH010/bHLH089/bHLH091, facilitate the nuclear distribution and enhance the in vivo function of DYT1 at anther stage 6 and onward (Figures 1D to 1F). When DYT1 was expressed in tobacco leaf cells alone, it was predominantly localized in the cytoplasm but weakly distributed in the nucleus (Figures 1D and 1F). However, in early stage 5 Arabidopsis anthers, DYT1 showed similarly strong signals in the nucleus and the cytoplasm (Figures 1A and 1B), before the expression of bHLH010/bHLH089/bHLH091 (Zhu et al., 2015), suggesting that other factors might also facilitate the nuclear localization of DYT1 at early anther stage 5. Our Y2H screen and BiFC results suggested that, in addition to bHLH010/bHLH089/bHLH091, DYT1 also interacts with five more bHLH transcription factors (Supplemental Data Set 1; Figure 1D). These five bHLH proteins are AMS (bHLH021), bHLH033 (ICE2), bHLH116 (ICE1), bHLH057, and bHLH125. Protein complexes of DYT1 and these five bHLHs were preferentially or specifically localized in the nucleus (Figure 1D). AMS acts downstream of DYT1, and no studies have revealed the function of ICE1, ICE2, bHLH057, and bHLH125 in anther development, especially in the early stages. However, publicly available microarray data (www.arabidopsis.org) indicate that these genes are expressed at the early flower stage (stage 9 flower and early inflorescences), suggesting that they may interact with DYT1 during these stages to facilitate the nuclear localization of DYT1.

METHODS

Plant Materials and Growth Conditions

Arabidopsis thaliana plants were grown under long-day conditions (16 h light/8 h in dark) in a 22°C growth room. All the Arabidopsis plants were in the Columbia (Col-0) ecotype background. The *Nicotiana benthamiana* plants were grown on soil under long-day conditions (16 h under light/8 h in dark) in a 22°C growth room for ~4 weeks before use.

Y2H Constructs and Analysis

Y2H screens were performed using a GAL4-based Matchmaker Gold Yeast Two-Hybrid System (Clontech). The *DYT1* coding region was amplified with primers oMF108 and oMF109 (Supplemental Data Set 6) and inserted into pGBKT7 with *Eco*RI and *Pst*I sites. The construct was confirmed by sequencing and then transformed into the Y2H gold yeast strain. Positive strains were mated with Y187 cells containing the Arabidopsis Matchmaker cDNA Library (Mate and Plate Library-Universal Arabidopsis, Normalized) in pGADT7 (Clontech). Screening and assays were performed following the manufacturer's instructions.

For verification of the interaction between various truncated DYT1 and bHLH proteins using the Y2H system, regions of the *DYT1* coding sequence were amplified with primers listed in Supplemental Data Set 6 and cloned separately into pGBKT7 with *Eco*RI and *Pst*I sites. The *AMS*, *bHLH010*, *bHLH089*, and *bHLH091* coding regions were amplified and inserted individually into pGADT7 with the *Nde*I and *Xho*I sites.

DYT1 point mutation constructs were generated using the Fast Mutagenesis System (Transgen) following the manufacturer's instructions, using primers listed in Supplemental Data Set 6. After verification by sequencing, the *DYT1* cDNAs carrying various mutations were amplified with primers oMF108 and oMF109 (Supplemental Data Set 6) and then ligated into the pGBKT7 with *Eco*RI and *Pst*I sites. Plasmids were transformed into the Y2H gold yeast strain for pGBKT7 constructs and the Y187 yeast strain for pGADT7 constructs using the LiAc/PEG method. The transformants were mated on the YPDA medium, and then the yeast containing both the bait and prey constructs was selected on SD/-Trp-Leu plates and re-streaked onto SD/-His-Ade-Trp-Leu with X-α-Gal and AbA plates to test for positive interactions.

Generation of Split-YFP and EYFP-Tagged Constructs and Transient Expression Analysis

DYT1 truncations were fused to pXY106 (nYFP-C), and *bHLH010*, *bHLH089*, and *bHLH091* were fused with pXY104 (N-cYFP) and transformed into *Agrobacterium tumefaciens* strain GV3101. Overnight cultures of Agrobacteria with an OD_{600} of ~1.2 to 2.0 were pelleted and resuspended in MES/$MgCl_2$/AS solution (10 mM MES, pH 5.6, 10 mM $MgCl_2$, and 0.5 mM acetosyringone) to a final OD_{600} of 2.0 each, and equal volumes of cells containing pXY106 and pXY104, respectively, were mixed and infiltrated into young *N. benthamiana* leaves. After ~36 to 48 h, YFP florescence, which suggested interaction between various protein pairs, was detected by an LSM-710 confocal microscope (Carl Zeiss MicroImaging).

bHLH010, *bHLH089*, and *bHLH091* coding regions were cloned into a 35S-C-EYFP binary vector pGWB441 (for subcellular localization analysis in Figure 1E), and *DYT1* was cloned into another 35S-N-EYFP binary vector pGWB442 (for subcellular localization analysis in Figures 1F, 3A, and 3B). The constructs were transformed into Agrobacterium strain GV3101, and bacterial cells were cultured overnight and resuspended in MES/$MgCl_2$/AS solution for transformation. The subcellular localizations of DYT1 and bHLH proteins were observed under the same microscope, and the nucleus was stained with 4′,6-diamidino-2-phenylindole (DAPI; Roche) at 10 μg/mL for ~20 min. Primers used for all constructs are listed in Supplemental Data Set 6.

Multiple Alignments

The homologous genes of *DYT1* were discovered with the HMM (Hidden Markov model) algorithm using the software hmmsearch (Eddy, 2011) in whole-genome sequenced species like rice (*Oryza sativa*) and poplar (*Populus trichocarpa*).

3D Structure Prediction

The 3D structure of $DYT1^{BIF}$ was predicted by the ab initio modeling method implemented in the Rosetta program (Bradley et al., 2005; Das and Baker, 2008). Five thousand independent structures were calculated, and that with the lowest Rosetta score (energy) was chosen for subsequent protein-protein docking to predict the homodimer structure of $DYT1^{BIF}$ by Rosetta (Chaudhury et al., 2011). In the docking calculation, 10,000 independent predictions were performed, and the predicted dimer with the lowest interface energy was used as the final 3D structure of the $DYT1^{BIF}$ homodimer (Figure 2G).

Generation of Transgenic Plants and Genotyping

To express the EYFP fusion proteins in vivo, the coding regions of DYT1 (amino acids 1 to 207), $DYT1^{\triangle BIF}$ (amino acids 1 to 124), $DYT1^{BIF}$, $mDYT1^{F139DL141D}$, $mDYT1^{I143DI144D}$, $DYT1^{N}$-$bHLH010^{BIF}$, and $DYT1^{N}$-$bHLH089^{BIF}$ were cloned into the pDONR/5*MYC vector that was modified based on pDONR/zeo (Supplemental Figure 12) and then into the pGWB41 binary vector, in which the 35S promoter was replaced by the 1.4-kb *DYT1* native promoter, using a LR reaction (Nakagawa et al., 2009). Primers used to construct transgenic plants are shown in Supplemental Data Set 6. All constructs were introduced into the *dyt1-3*/+ heterozygous background by Agrobacterium-mediated transformation following the floral dipping method (Clough and Bent, 1998). All transgenic lines were screened on solid 0.5× MS medium (0.4% Phytagel and 25 mg/mL hygromycin), and

positive lines were transferred to soil. The genotype of *dyt1-3* mutant plants was verified with primers listed in Supplemental Data Set 7.

Characterization of Plant Phenotypes

Phenotypes of transgenic plants for each construct were verified in at least three independent lines. Flowers were photographed using a Stereo Discovery V8 dissecting microscope (Carl Zeiss MicroImaging) with a Spot Flex digital camera (Diagnostic Instruments). To determine pollen viability, stage 12 anthers (Sanders et al., 1999) were collected and stained with the Alexander solution (Alexander, 1969) and photographed under an AXIO Scope A1 microscope (Carl Zeiss MicroImaging) with an Axio Cam HRc camera (Carl Zeiss MicroImaging).

Electrophoretic Mobility Shift Assay

Various DYT1 proteins and bHLH089 protein were expressed in *Escherichia coli* using the pGEX4T-1 (GE) and pCold-TF (Takara) expression system, as described in the manufacturer's instructions. GST- and His-tagged proteins were purified by GST or Ni-affinity chromatography, and the concentrations were confirmed by SDS-PAGE followed by Coomassie Brilliant Blue staining. Single-strand biotin-labeled oligonucleotides were synthesized by Invitrogen and annealed to double-stranded DNA probes according to the manufacturer's instructions. The in vitro binding experiments were performed according to the Light Shift Chemiluminescent EMSA system (Thermo). Equal amounts of DYT1 and bHLH089 proteins were used in the heterodimer DNA binding reactions.

Transient Transcription Dual-Luciferase Assays

Coding regions of *DYT1* truncations, mutated *DYT1*, and native *bHLH010/089/091* were cloned into the pGWB441 binary vector. The promoter sequences of *MS1* and *MYB35* were PCR amplified and inserted into the pGreenII-0800-LUC vector. After sequencing, all the constructs were transformed into GV3101 Agrobacteria, while the pGreenII constructs were cotransformed with pSoup-P19. The mixture of cells containing constructs with protein and promoter was infiltrated according to the published method (Hellens et al., 2005). The luciferase activity of *N. benthamiana* extracts was analyzed using a Dual-Luciferase Assay Kit (Promega) and then detected by a Synergy 2 multimode microplate (Bio-Tek) as described previously (Hellens et al., 2005).

Real-Time PCR Analysis

To detect the expression level of *DYT1* and other downstream genes, flower buds of transgenic plants were collected and total RNA was extracted according to a Trizol-based (Sigma) method. After DNaseI (Thermo) digestion, a reverse transcription system (Promega) was used for first-strand cDNA synthesis. Real-time PCR was performed with SYBR premix Ex Taq II (Takara) on the ABI StepOnePlus real-time system (Life Technologies). Primers are listed in Supplemental Data Set 8, and EF1α (AT5G60390) was used as an internal control to normalize the gene expression level.

Accession Numbers

Sequence data from this article can be found in the GenBank/EMBL databases under the following accession numbers: *DYT1* (AT4G21330, NM_118253); *bHLH010* (AT2G31220, NM_128678); *bHLH089* (AT1G06170, NM_100498); *bHLH091* (AT2G31210, NM_128677); *EF1a* (AT5G60390, AK318784); *MS1* (AT5G22260, NM_122131); *MYB35* (AT3G28470, NM_113767); *MYB80/MYB103* (AT5G56110, NM_124993); *MYB99* (AT5G62320, NM_125626); *AMS* (AT2G16910, NM_127244); *bHLH033* (AT1G12860, NM_101157); *bHLH116* (AT3G26744, NM_113586); *bHLH057* (AT4G01460, NM_116376); and *bHLH125* (AT1G62975, NM_148621).

Supplemental Data

Supplemental Figure 1. Phenotypic analyses of the *DYT1-GR* transgenic plants and anthers before and after DEX induction.

Supplemental Figure 2. Statistical analyses of the subcellular localization pattern of DYT1-EYFP in tapetal cells at anther stage 5-7.

Supplemental Figure 3. Functional enrichment of the 143 DYT1-ineraction candidates from screens using yeast two-hybrid system.

Supplemental Figure 4. The amino acid alignment of DYT1 and several angiosperm DYT1 orthologs.

Supplemental Figure 5. The BIF domain is important for the dimerization of DYT1.

Supplemental Figure 6. Y2H results showing interactions between various mutated DYT1, DYT1, bHLH010, bHLH089, and bHLH091 proteins.

Supplemental Figure 7. Immunoblot analysis of expression of various DYT1 proteins in yeast.

Supplemental Figure 8. Real time-PCR results to show the expression level of DYT1 in transgenic plants with various mutation and truncations.

Supplemental Figure 9. Real-time PCR results showing the expression level of the $DYT1^{BIF}$ in *DYT1:DYT1^{BIF}-EYFP*/WT plants.

Supplemental Figure 10. Amino acid sequence comparison between DYT1, bHLH010, bHLH089, and bHLH091.

Supplemental Figure 11. RNA expression levels of chimeric transgenes.

Supplemental Figure 12. Schematic maps of constructs to express various DYT1 proteins under the control of pGWB41-DYT1pro.

Supplemental Data Set 1. List of the putative DYT1 interaction proteins screened in this study.

Supplemental Data Set 2. The cell numbers observed in each of the subcellular localization analyses in tobacco leaves.

Supplemental Data Set 3. The distribution of BIF domain-containing bHLH transcription factors in Arabidopsis bHLH family.

Supplemental Data Set 4. A list of genes used for BIF domain analyses.

Supplemental Data Set 5. Line numbers of each transgene observed in this study and male fertility phenotype of each transgenic line.

Supplemental Data Set 6. Primers for constructs in this work.

Supplemental Data Set 7. Primers for *dyt1-3* genotyping.

Supplemental Data Set 8. Primers for real-time PCR.

ACKNOWLEDGMENTS

This work was supported by grants from the Ministry of Science and Technology of the People's Republic of China (2012CB910503) and the National Natural Science Foundation of China (31130006 and 31470282).

AUTHOR CONTRIBUTIONS

J.C., F.C., and H.M. designed the research. J.C. performed the BiFC, the EMSA, and the real-time PCR experiments, generated the transgenic lines, and performed the phenotypic observation. C.Y. carried out the multiple alignments and phylogenetic analysis. C.Y. and J.C. together conducted

the site-directed mutagenesis, the Y2H experiments, and the subcellular localization observations. E.Z. generated constructs for the BiFC assay. Q.H. did the 3D structure prediction for the BIF homodimer. J.C., C.Y., F.C., and H.M. analyzed the data and wrote the article.

Received November 23, 2015; revised March 2, 2016; accepted April 23, 2016; published April 25, 2016.

REFERENCES

Alexander, M.P. (1969). Differential staining of aborted and non-aborted pollen. Stain Technol. **44:** 117–122.

Bhave, N.S., Veley, K.M., Nadeau, J.A., Lucas, J.R., Bhave, S.L., and Sack, F.D. (2009). TOO MANY MOUTHS promotes cell fate progression in stomatal development of *Arabidopsis* stems. Planta **229:** 357–367.

Bradley, P., Misura, K.M., and Baker, D. (2005). Toward high-resolution de novo structure prediction for small proteins. Science **309:** 1868–1871.

Castillon, A., Shen, H., and Huq, E. (2007). Phytochrome Interacting Factors: central players in phytochrome-mediated light signaling networks.Trends Plant Sci. **12:** 514–521.

Chang, A.T., Liu, Y., Ayyanathan, K., Benner, C., Jiang, Y., Prokop, J.W., Paz, H., Wang, D., Li, H.R., Fu, X.D., RauscherIII, F.J., and Yang, J. (2015). An evolutionarily conserved DNA architecture determines target specificity of the TWIST family bHLH transcription factors. Genes Dev. **29:** 603–616.

Chaudhury, S., Berrondo, M., Weitzner, B.D., Muthu, P., Bergman, H., and Gray, J.J. (2011). Benchmarking and analysis of protein docking performance in Rosetta v3.2. PLoS One **6:** e22477.

Clough, S.J., and Bent, A.F. (1998). Floral dip: a simplified method for *Agrobacterium*-mediated transformation of *Arabidopsis thaliana.* Plant J. **16:** 735–743.

Das, R., and Baker, D. (2008). Macromolecular modeling with rosetta. Annu. Rev. Biochem. **77:** 363–382.

Eddy, S.R. (2011). Accelerated profile HMM searches. PLOS Comput. Biol. **7:** e1002195.

Ellenberger, T., Fass, D., Arnaud, M., and Harrison, S.C. (1994). Crystal structure of transcription factor E47: E-box recognition by a basic region helix-loop-helix dimer. Genes Dev. **8:** 970–980.

Feng, B., Lu, D., Ma, X., Peng, Y., Sun, Y., Ning, G., and Ma, H. (2012). Regulation of the *Arabidopsis* anther transcriptome by DYT1 for pollen development. Plant J. **72:** 612–624.

Friedrichsen, D.M., Nemhauser, J., Muramitsu, T., Maloof, J.N., Alonso, J., Ecker, J.R., Furuya, M., and Chory, J. (2002). Three redundant brassinosteroid early response genes encode putative bHLH transcription factors required for normal growth. Genetics **162:** 1445–1456.

Fu, Z., Yu, J., Cheng, X., Zong, X., Xu, J., Chen, M., Li, Z., Zhang, D., and Liang, W. (2014). The rice basic helix-Loop-helix transcription factor TDR INTERACTING PROTEIN2 is a central switch in early anther development. Plant Cell **26:** 1512–1524.

Grant, G.A. (2006). The ACT domain: a small molecule binding domain and its role as a common regulatory element. J. Biol. Chem. **281:** 33825–33829.

Gu, J.N., Zhu, J., Yu, Y., Teng, X.D., Lou, Y., Xu, X.F., Liu, J.L., and Yang, Z.N. (2014). DYT1 directly regulates the expression of *TDF1* for tapetum development and pollen wall formation in *Arabidopsis.* Plant J. **80:** 1005–1013.

Hellens, R.P., Allan, A.C., Friel, E.N., Bolitho, K., Grafton, K., Templeton, M.D., Karunairetnam, S., Gleave, A.P., and Laing, W.A. (2005). Transient expression vectors for functional genomics, quantification of promoter activity and RNA silencing in plants. Plant Methods **1:** 13.

Huffman, J.L., Mokashi, A., Bächinger, H.P., and Brennan, R.G. (2001). The basic helix-loop-helix domain of the aryl hydrocarbon receptor nuclear transporter (ARNT) can oligomerize and bind E-box DNA specifically. J. Biol. Chem. **276:** 40537–40544.

Ji, C., Li, H., Chen, L., Xie, M., Wang, F., Chen, Y., and Liu, Y.G. (2013). A novel rice bHLH transcription factor, DTD, acts coordinately with TDR in controlling tapetum function and pollen development. Mol. Plant **6:** 1715–1718.

Ju, C., et al. (2012). CTR1 phosphorylates the central regulator EIN2 to control ethylene hormone signaling from the ER membrane to the nucleus in Arabidopsis. Proc. Natl. Acad. Sci. USA **109:** 19486–19491.

Jung, K.H., Han, M.J., Lee, Y.S., Kim, Y.W., Hwang, I., Kim, M.J., Kim, Y.K., Nahm, B.H., and An, G. (2005). *Rice Undeveloped Tapetum1* is a major regulator of early tapetum development.Plant Cell **17:** 2705–2722.

Kanaoka, M.M., Pillitteri, L.J., Fujii, H., Yoshida, Y., Bogenschutz, N.L., Takabayashi, J., Zhu, J.K., and Torii, K.U. (2008). *SCREAM/ICE1* and *SCREAM2* specify three cell-state transitional steps leading to *arabidopsis* stomatal differentiation. Plant Cell **20:** 1775–1785.

Kim, T.W., Guan, S., Sun, Y., Deng, Z., Tang, W., Shang, J.X., Sun, Y., Burlingame, A.L., and Wang, Z.Y. (2009). Brassinosteroid signal transduction from cell-surface receptor kinases to nuclear transcription factors. Nat. Cell Biol. **11:** 1254–1260.

Lamb, P., and McKnight, S.L. (1991). Diversity and specificity in transcriptional regulation: the benefits of heterotypic dimerization. Trends Biochem. Sci. **16:** 417–422.

Leivar, P., Monte, E., Oka, Y., Liu, T., Carle, C., Castillon, A., Huq, E., and Quail, P.H. (2008). Multiple phytochrome-interacting bHLH transcription factors repress premature seedling photomorphogenesis in darkness. Curr. Biol. **18:** 1815–1823.

Li, S. (2014). Transcriptional control of flavonoid biosynthesis: fine-tuning of the MYB-bHLH-WD40 (MBW) complex. Plant Signal. Behav. **9:** e27522.

Liu, H., Yu, X., Li, K., Klejnot, J., Yang, H., Lisiero, D., and Lin, C. (2008). Photoexcited CRY2 interacts with CIB1 to regulate transcription and floral initiation in *Arabidopsis.* Science **322:** 1535–1539.

Liu, J.X., Srivastava, R., Che, P., and Howell, S.H. (2007). An endoplasmic reticulum stress response in Arabidopsis is mediated by proteolytic processing and nuclear relocation of a membrane-associated transcription factor, bZIP28. Plant Cell **19:** 4111–4119.

Ma, P.C., Rould, M.A., Weintraub, H., and Pabo, C.O. (1994). Crystal structure of MyoD bHLH domain-DNA complex: perspectives on DNA recognition and implications for transcriptional activation. Cell **77:** 451–459.

McGonigle, B., Bouhidel, K., and Irish, V.F. (1996). Nuclear localization of the Arabidopsis APETALA3 and PISTILLATA homeotic gene products depends on their simultaneous expression. Genes Dev. **10:** 1812–1821.

Nadeau, J.A. (2009). Stomatal development: new signals and fate determinants. Curr. Opin. Plant Biol. **12:** 29–35.

Nakagawa, T., Ishiguro, S., and Kimura, T. (2009). Gateway vectors for plant transformation. Plant Biotechnol. J. **26:** 275–284.

Nayar, S., Kapoor, M., and Kapoor, S. (2014). Post-translational regulation of rice MADS29 function: homodimerization or binary interactions with other seed-expressed MADS proteins modulate its translocation into the nucleus. J. Exp. Bot. **65:** 5339–5350.

Niu, N., Liang, W., Yang, X., Jin, W., Wilson, Z.A., Hu, J., and Zhang, D. (2013). EAT1 promotes tapetal cell death by regulating aspartic

proteases during male reproductive development in rice. Nat. Commun. **4:** 1445.

Pires, N., and Dolan, L. (2010). Origin and diversification of basic-helix-loop-helix proteins in plants. Mol. Biol. Evol. **27:** 862–874.

Qiao, H., Shen, Z., Huang, S.S., Schmitz, R.J., Urich, M.A., Briggs, S.P., and Ecker, J.R. (2012). Processing and subcellular trafficking of ER-tethered EIN2 control response to ethylene gas. Science **338:** 390–393.

Sanders, P.M., Bui, A.Q., Weterings, K., McIntire, K.N., Hsu, Y.-C., Lee,P.Y., Truong, M.T., Beals, T.P., and Goldberg, R.B. (1999). Anther developmental defects in *Arabidopsis thaliana* male-sterile mutants. Sex. Plant Reprod. **11:** 297–322.

Serna, L. (2009a). Emerging parallels between stomatal and muscle cell lineages. Plant Physiol. **149:** 1625–1631.

Serna, L. (2009b). Cell fate transitions during stomatal development. BioEssays **31:** 865–873.

Shin, J., Kim, K., Kang, H., Zulfugarov, I.S., Bae, G., Lee, C.H., Lee, D., and Choi, G. (2009). Phytochromes promote seedling light responses by inhibiting four negatively-acting phytochrome-interacting factors. Proc. Natl. Acad. Sci. USA **106:** 7660–7665.

Sorensen, A.M., Kröber, S., Unte, U.S., Huijser, P., Dekker, K., and Saedler, H. (2003). The *Arabidopsis ABORTED MICROSPORES* (*AMS*) gene encodes a MYC class transcription factor. Plant J. **33:** 413–423.

Xu, J., Ding, Z., Vizcay-Barrena, G., Shi, J., Liang, W., Yuan, Z., Werck-Reichhart, D., Schreiber, L., Wilson, Z.A., and Zhang, D. (2014). *ABORTED MICROSPORES* acts as a master regulator of pollenwall formation in *Arabidopsis.* Plant Cell **26:** 1544–1556.

Zhang, L.Y., et al. (2009). Antagonistic HLH/bHLH transcription factors mediate brassinosteroid regulation of cell elongation and plant development in rice and *Arabidopsis.* Plant Cell **21:** 3767–3780.

Zhang, W., Sun, Y., Timofejeva, L., Chen, C., Grossniklaus, U., and Ma, H. (2006). Regulation of *Arabidopsis* tapetum development and function by *DYSFUNCTIONAL TAPETUM1* (*DYT1*) encoding a putative bHLH transcription factor. Development **133:** 3085–3095.

Zhang, Y., Mayba, O., Pfeiffer, A., Shi, H., Tepperman, J.M., Speed, T.P., and Quail, P.H. (2013). A quartet of PIF bHLH factors provides a transcriptionally centered signaling hub that regulates seedling morphogenesis through differential expression-patterning of shared target genes in *Arabidopsis.* PLoS Genet. **9:** e1003244.

Zhao, M., Morohashi, K., Hatlestad, G., Grotewold, E., and Lloyd, A. (2008). The TTG1-bHLH-MYB complex controls trichome cell fate and patterning through direct targeting of regulatory loci. Development **135:** 1991–1999.

Zhu, E., You, C., Wang, S., Cui, J., Niu, B., Wang, Y., Qi, J., Ma, H., and Chang, F. (2015). The DYT1-interacting proteins bHLH010, bHLH089 and bHLH091 are redundantly required for Arabidopsis anther development and transcriptome. Plant J. **83:** 976–990.